



Article

# A Facile In Situ Synthesis of Resorcinol-Mediated Silver Nanoparticles and the Fabrication of Agar-Based Functional Nanocomposite Films

Yeong-Ju Bang<sup>1</sup>, Swarup Roy<sup>1,2</sup>  and Jong-Wan Rhim<sup>1,\*</sup> 

<sup>1</sup> Department of Food and Nutrition, BioNanocomposite Research Center, Kyung Hee University, 26 Kyungheedaero-ro, Dongdaemun-gu, Seoul 02447, Korea; byjsky1004@hanmail.net (Y.-J.B.); swaruproy2013@gmail.com (S.R.)

<sup>2</sup> School of Bioengineering and Food Technology, Shoolini University, Solan 173229, India

\* Correspondence: jwrhim@khu.ac.kr

**Abstract:** The in situ synthesis of silver nanoparticles (AgNPs) was performed using resorcinol and agar to produce agar-based antioxidant and antimicrobial films. AgNPs were regularly dispersed on the film matrix, and their presence improved the thermal stability of films. Additionally, the addition of AgNPs slightly increased the agar-based film's tensile strength (~10%), hydrophobicity (~40%), and water vapor barrier properties (~20%) at 1.5 wt% of AgNP concentration. The resorcinol also imparted UV-barrier and antioxidant activity to the agar-based film. In particular, the agar-based film containing a higher quantity of AgNPs (>1.0 wt%) was highly effective against the foodborne pathogenic bacteria *L. monocytogenes* and *E. coli*. Therefore, agar-based composite films with improved physicochemical and functional properties may be promising for active packaging.

**Keywords:** agar; resorcinol; AgNP; bionanocomposite; antibacterial and antioxidant activity



**Citation:** Bang, Y.-J.; Roy, S.; Rhim, J.-W. A Facile In Situ Synthesis of Resorcinol-Mediated Silver Nanoparticles and the Fabrication of Agar-Based Functional Nanocomposite Films. *J. Compos. Sci.* **2022**, *6*, 124. <https://doi.org/10.3390/jcs6050124>

Academic Editor: Francesco Tornabene

Received: 2 April 2022

Accepted: 22 April 2022

Published: 24 April 2022

**Publisher's Note:** MDPI stays neutral with regard to jurisdictional claims in published maps and institutional affiliations.



**Copyright:** © 2022 by the authors. Licensee MDPI, Basel, Switzerland. This article is an open access article distributed under the terms and conditions of the Creative Commons Attribution (CC BY) license (<https://creativecommons.org/licenses/by/4.0/>).

## 1. Introduction

Nanotechnology has a significant impact on all industries, and the size of the industry is expected to reach USD 3 trillion worldwide by 2020 [1,2]. From agriculture to food processing to food packaging, the application of nanotechnology in the food industry is increasing [3,4]. Packaging is undoubtedly the most attractive research area in food science, and one of the main functions of food packaging is to protect and preserve food quality and reduce food waste [5–8]. In particular, the functional nanocomposite packaging material containing functional nanomaterials is expected to dramatically improve the lifespan of packaged food by securing the safety of packaged food and improving the quality of food [9–12]. To this end, antimicrobial nanoparticles are a promising area of current research for developing active food packaging films.

Several functional metal nanoparticles, such as copper, silver, titanium, and zinc, are particularly interesting in food packaging applications [13,14]. Silver nanoparticles (AgNPs) have been considered the most interesting because of their broad antimicrobial activity against foodborne pathogens [15]. In addition, the unique optical, catalytic, and electrical properties and the high thermal stability of AgNPs make them more suitable for food packaging applications [16]. Additionally, it is known that the antibacterial activity of AgNPs is affected by many factors [17]. Therefore, to fully exhibit the properties of AgNPs, AgNPs must be evenly dispersed on the surface of the film matrix without aggregation. Recently, various green methods have been used for the preparation of AgNPs using different biobased reducing agents, such as biopolymers [18], bacteria [19], fungi [20,21], and plant extract [22–24].

In this regard, resorcinol is one of the exciting biomaterials for AgNP synthesis. Resorcinol (C<sub>6</sub>H<sub>4</sub>(OH)<sub>2</sub>) is 1,3-dihydroxybenzene that has been used in a variety of applications,

such as cosmetics, pharmaceuticals, antioxidants, and dyes [25]. As per MSDS, resorcinol has a moderate health risk index [26]. Therefore, resorcinol can be used as a stabilizing and reducing agent for synthesizing AgNPs. In addition, resorcinol composed of phenolic groups can improve the film's mechanical properties by providing an opportunity to form intermolecular interactions with polymers by hydrogen bonding [27]. The phenolic compounds of resorcinol may also expand the uses of food packing films by inducing functional properties [28].

On the other hand, concerns about environmental pollution due to the accumulation of non-degradable, oil-based synthetic plastic packaging materials are growing [29,30]. The use of plastics in food packaging is increasing every year, with a growth rate of ~12% per year [1,2]. Therefore, replacing them with biopolymers has become a significant challenge for the packaging industry [4]. For this purpose, various biopolymers have been used to develop biodegradable packaging materials because of their biodegradability, renewability, environmental friendliness, and sustainability [31–33]. The inherent problems of biopolymer-based films, such as low mechanical properties and hydrophilicity, can be improved by making composite films with nanoparticles, such as AgNPs, and providing additional functions, such as antibacterial and antioxidant properties [31]. Polysaccharides are most attractive for food packaging applications among biopolymers due to their superior mechanical and film-forming properties compared to other biopolymer materials [32]. In this context, agar, a polysaccharide derived from marine algae, such as *Gracilaria* and *Gelidium*, has been widely used to manufacture biodegradable functional packaging films. Agar is composed of alternating D-galactose and 3, 6-anhydro-L-galactopyranose units [34]. Agar is known to have sufficient water-resistant properties and good mechanical strength suitable for food packaging applications [35]. Agar has been used to prepare functional composite films by adding AgNPs [18,36–39]. Previously, resorcinol and gelatin were used to prepare silver nanocomposite films [26], but, to our knowledge, there are no reports of the in situ synthesis of agar-based functional composite films integrated with resorcinol-reduced AgNPs.

Therefore, the objective of this work is to synthesize AgNPs using resorcinol and fabricate functional agar-based nanocomposite films.

## 2. Materials and Methods

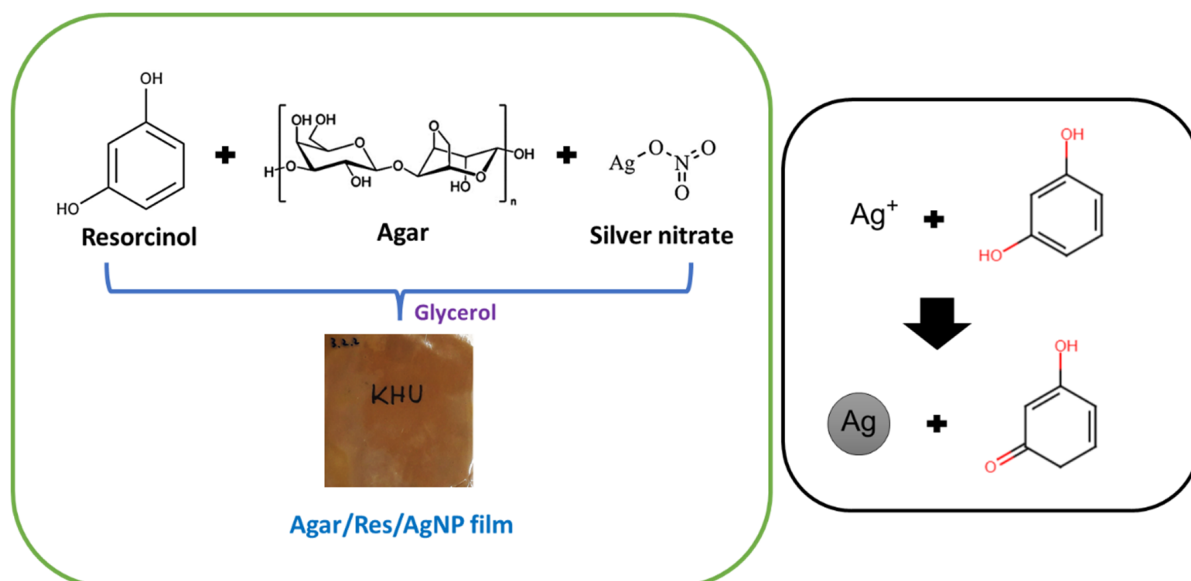
### 2.1. Materials

Food grade agar was obtained from Gel-Tec Co., Ltd. (Seoul, Korea). Resorcinol ( $C_6H_6O_2$ , 99%), ABTS (2,2'-azino-bis(3-ethylbenzothiazoline-6-sulphonic acid)), DPPH (2,2-diphenyl-1-picrylhydrazyl), and methanol (99.8%) were procured from Sigma-Aldrich (St. Louis, MO, USA). Silver nitrate was purchased from Daejung Chemicals & Materials Co., Ltd. (Siheung, Gyeonggi-do, Korea).

#### 2.1.1. Preparation of Films

Agar/resorcinol/AgNP nanocomposite films were prepared using the solution casting method [26]. First, silver nitrate ( $AgNO_3$ ) and resorcinol stock solutions were prepared by dissolving 1.0 g of each component in 10 mL of distilled water. For the preparation of AgNP, 1.0 g of agar was first dissolved in 200 mL of distilled water, and then 3 mL of resorcinol (0.1 g) solution (10 wt% based on agar) was added. Then, various amounts of  $AgNO_3$  stock solution (0.15, 0.3, and 0.45 mL corresponding to 0.5, 1.0, and 1.5 wt% of  $AgNO_3$  based on agar) were added slowly into the solution and heated at 85 °C for 4 h with vigorous stirring. Then, 2 g of agar and 0.9 g of glycerol (30 wt% based on agar) were added slowly to the above mixture and heated at 95 °C for another 20 min with vigorous stirring. The film-forming solution was cast on the leveled Teflon film-coated glass plate. The neat agar and agar/resorcinol films were prepared following the same procedure without AgNP. The prepared films were designated Agar, Agar/Res, Agar/Res/AgNP<sup>0.5%</sup>, Agar/Res/AgNP<sup>1%</sup>, and Agar/Res/AgNP<sup>1.5%</sup> according to the component and AgNP concentration. Detailed methods of the characterization and measurement of the film properties are provided in

the Supporting Materials. The procedure for fabricating Agar/Res/AgNP composite films is shown schematically in Scheme 1.



**Scheme 1.** Fabrication of the Agar/Res/AgNP composite films.

### 2.1.2. Characterization and Properties of the Films SEM and FT-IR

The surface morphology of the composite films was tested using a field emission scanning electron microscope (FE-SEM, S-4800, Hitachi Co., Ltd., Matsuda, Japan) at an accelerating voltage of 2 kV.

The attenuated total reflectance-Fourier transform infrared (AT-FTIR) spectrophotometer (SENSOR 37 Spectrophotometer, Billerica, MA, USA) was used to measure the chemical structure.

#### Surface Color and Optical Properties

The surface color of the composite films was analyzed using a Chroma meter (Konica Minolta, CR-400, Tokyo, Japan). The total color difference ( $\Delta E$ ) was calculated with the following equation:

$$\Delta E = \sqrt{(\Delta L)^2 + (\Delta a)^2 + (\Delta b)^2}, \quad (1)$$

where  $\Delta L$ ,  $\Delta a$ , and  $\Delta b$  are the differences between the color of standard color plate and film samples.

The light absorption spectra of the nanocomposite films were determined over a range of 200–700 nm using a UV-visible spectrophotometer (Mecasys Optizen POP Series UV/Vis, Seoul, Korea). In addition, the UV-light barrier property and transparency of the film were determined by measuring the percent transmittance at 280 nm ( $T_{280}$ ) and 660 nm ( $T_{660}$ ), respectively [11].

#### Mechanical Properties

The Instron Universal Testing Machine (Model 5565, Instron Engineering Corporation, Canton, MA, USA) was used to determine the mechanical properties [12].

#### Water Contact Angle (WCA) and Water Vapor Permeability (WVP)

The water contact angle (WCA) of the film was measured using a WCA analyzer (model Phoenix 150, Surface Electro Optics Co., Ltd., Kunpo, Korea). About 10  $\mu\text{L}$  of distilled water was placed on the surface of the film using a micro-syringe [26].

The water vapor permeability (WVP) of the film was determined following the standard method of ASTM E96-95 with modifications. Each film was placed on the top of WVP cup filled with distilled water. The WVP cups were stored in a humidity chamber controlled at 25 °C and 50% relative humidity (RH). The weight of the cups was obtained at 1 h intervals for 8 h. The water vapor transmission rate (WVTR) was determined from the slope of the weight loss plot of the WVP cup versus time, and the WVP ( $\text{g}\cdot\text{m}/\text{m}^2\cdot\text{s}\cdot\text{Pa}$ ) of the film was calculated as follows:

$$\text{WVP} = (\text{WVTR} \times L) / \Delta p, \quad (2)$$

where  $L$  was the mean film thickness and  $\Delta p$  was the water vapor pressure difference (Pa) across the film.

#### Thermogravimetric Analysis

Thermogravimetric analysis (TGA) was conducted using a thermogravimetric analyzer (Hi-Res TGA 2950, TA Instrument, New Castle, DE, USA). The samples were heated from 30 °C to 600 °C with a 10 °C/min heating rate under a nitrogen flow of 50 mL/min.

#### Antioxidant Activity

The antioxidant activities of the films were measured by assessing the free radical scavenging activity [11]. The 2,2-diphenyl-1-picrylhydrazyl radical (DPPH $\bullet$ ) and 2,2'-azino-bis(3-ethylbenzothiazoline-6-sulfonic acid) (ABTS $\bullet^+$ ) radical scavenging methods were used for the antioxidant activity assessment. For the DPPH analysis, a prescribed amount of the methanolic solution of DPPH was freshly made, and ~100 mg of tested film sample was added in a 10 mL DPPH solution and incubated at room temperature for 30 min and measured the absorbance at 517 nm. For the ABTS assay, a prescribed amount of potassium sulfate was added to the ABTS solution, followed by overnight incubation in the dark to make the ABTS assay solution. A total of ~100 mg of the tested film samples were added to 10 mL of ABTS assay solution, incubated at room temperature for 30 min, and measured the absorbance at 734 nm. The antioxidative activity was calculated as follows:

$$\text{Free radical scavenging activity (\%)} = \frac{A_c - A_t}{A_c} \times 100, \quad (3)$$

where  $A_c$  and  $A_t$  are the absorbances of DPPH/ABTS of the control and test film, respectively. The test was performed in triplicate, and the average value was reported.

#### Antimicrobial Activity

The antimicrobial activity of the agar-based composite film was examined using a viable colony count method against two types of foodborne pathogenic bacteria, *L. monocytogenes* and *Escherichia coli* [26]. The test strains were inoculated in 20 mL of BHI and TSB broth, respectively, for 16 h at 37 °C. Next, 200  $\mu\text{L}$  of diluted inoculum ( $10^8$ – $10^9$  CFU/mL) was transferred to 20 mL of fresh BHI and TSB broth containing a 100 mg film sample. The flask was stored in a shaker at 37 °C for 12 h. Samples were taken at intervals of 3 h, and bacterial colonies were counted to measure each pathogen's cell viability.

#### Statistical Analysis

One-way analysis of variance (ANOVA) was performed, and the significant differences among the film properties were determined ( $p < 0.05$ ) with Duncan's multiple range tests using the SPSS statistical analysis program (SPSS 21, SPSS Inc., Chicago, IL, USA).

### 3. Results and Discussion

#### 3.1. Surface Color and Optical Properties

The apparent shape of the agar-based film is shown in Figure 1a. All films were flexible and standalone. The neat agar film was colorless and transparent, while the resorcinol-containing film showed a slight yellow tint. When AgNP was incorporated, the color of the film changed to yellowish-brown and dark brown depending on the concentration of AgNP. As shown in Scheme 1, the resorcinol-mediated AgNP was most likely formed through one-electron oxidation steps [28].

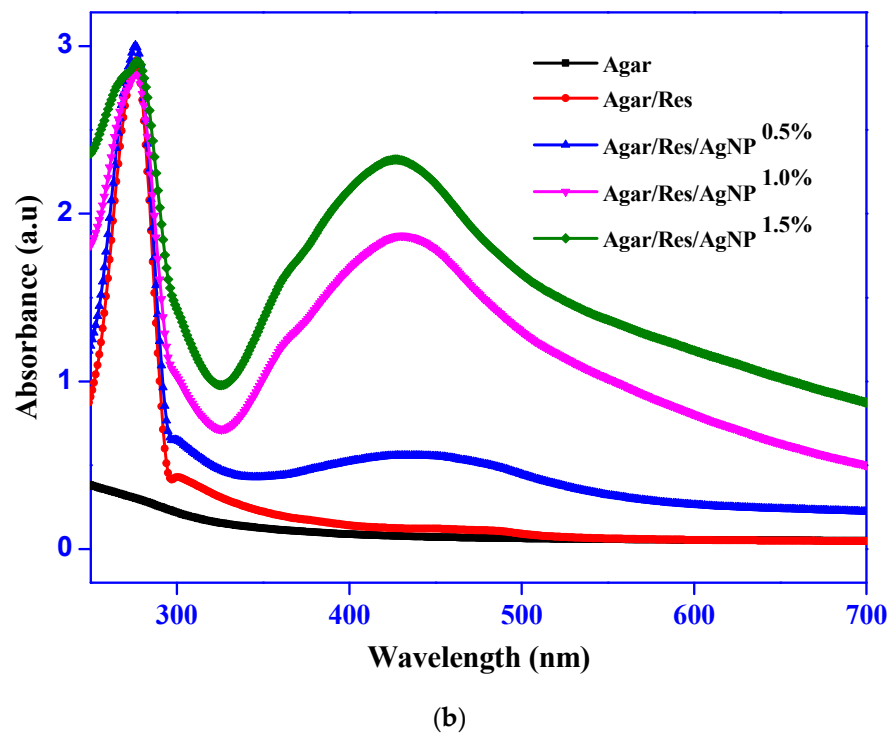
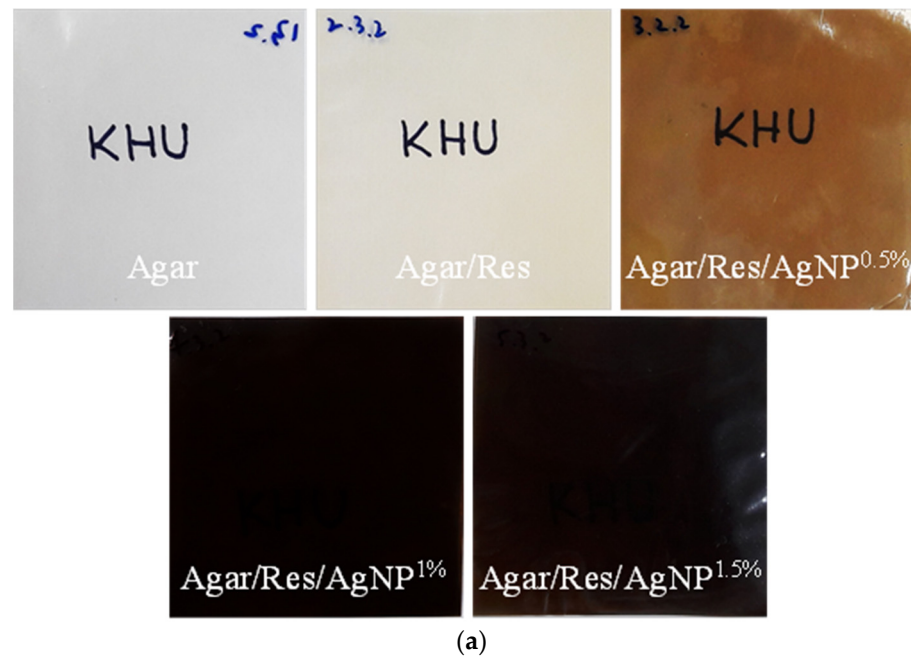


**Figure 1.** Appearance (a) and UV-visible light absorption spectra (b) of the agar-based composite films.

The light absorption spectra of the agar-based films are shown in Figure 1b. The neat agar film did not show any specific light absorption. However, the agar film showed a strong light absorption peak at 280 nm due to UV absorption by the phenolic compound of resorcinol [28,40]. On the other hand, the Agar/Res/AgNP films exhibited another unique light absorption peak around 430–440 nm, which is characteristic of AgNPs [41]. In addition, the peak intensity increased significantly with increasing AgNP concentration. This peak is attributed to the surface plasmon resonance (SPR) transition of AgNPs, confirming that AgNPs were successfully prepared by resorcinol [42]. Similarly, Ahmed, Saifullah, Ahmad, Swami, and Ikram (2016) also confirmed the formation of AgNPs using *Azadirachta indica* aqueous leaf extract [43].

The effects of resorcinol and AgNPs on the color of composite films were determined using Hunter *L*, *a*, *b*-values (Table 1). The neat agar film showed a high *L*-value (lightness, >90) with low *a*- and *b*-values (redness and yellowness, respectively). The addition of resorcinol did not significantly affect the *L*-value and *a*-value of the agar film ( $p > 0.05$ ). Still, the *b*-value was significantly increased ( $p < 0.05$ ) due to the yellow color of resorcinol. When AgNP was incorporated, the lightness (*L*-value) of the film decreased considerably depending on the concentration of AgNP, while the *a*-value (redness) and *b*-value (yellowness) increased significantly. The significant changes in the *L*, *a*, and *b* values of the Agar/Res/AgNP films were due to the formation of AgNPs, which gave the films a brown tint [26,44]. The *b*-values of the Agar/Res/AgNP films were very high when a small amount of AgNP (0.5 wt%) was added, but decreased significantly when a higher amount of AgNP (>1.0 wt%) was added. The abrupt color change of the Agar/Res/AgNP films is probably because the color of AgNPs was yellow at a low concentration, but became dark brown when the AgNP concentration increased above 1.0 wt%. As a result, the total color difference ( $\Delta E$ ) of the agar-based composite films increased significantly due to resorcinol and AgNP. The similar effects of resorcinol and AgNPs on the color properties were observed for gelatin-based films [26].

**Table 1.** Surface color and light transmittance of the agar-based composite films.

Films	<i>L</i>	<i>a</i>	<i>b</i>	$\Delta E$	T <sub>280</sub> (%)	T <sub>660</sub> (%)
Agar	91.0 ± 0.2 <sup>d</sup>	−0.6 ± 0.1 <sup>a</sup>	6.8 ± 0.1 <sup>a</sup>	2.5 ± 0.1 <sup>a</sup>	53.8 ± 1.0 <sup>b</sup>	89.5 ± 0.2 <sup>d</sup>
Agar/Res	90.3 ± 0.3 <sup>d</sup>	−0.5 ± 0.1 <sup>a</sup>	9.5 ± 0.4 <sup>c</sup>	5.2 ± 0.5 <sup>b</sup>	0.2 ± 0.1 <sup>a</sup>	89.0 ± 0.3 <sup>d</sup>
Agar/Res/AgNP <sup>0.5%</sup>	57.3 ± 0.9 <sup>c</sup>	4.2 ± 0.6 <sup>b</sup>	41.5 ± 1.0 <sup>d</sup>	51.4 ± 1.3 <sup>c</sup>	0.1 ± 0.1 <sup>a</sup>	57.3 ± 1.1 <sup>c</sup>
Agar/Res/AgNP <sup>1.0%</sup>	35.8 ± 0.9 <sup>b</sup>	8.1 ± 0.7 <sup>c</sup>	9.8 ± 0.6 <sup>c</sup>	57.1 ± 0.9 <sup>d</sup>	0.1 ± 0.1 <sup>a</sup>	29.1 ± 1.3 <sup>b</sup>
Agar/Res/AgNP <sup>1.5%</sup>	31.4 ± 0.8 <sup>a</sup>	9.7 ± 1.0 <sup>d</sup>	8.5 ± 0.4 <sup>b</sup>	61.3 ± 0.8 <sup>e</sup>	0.1 ± 0.1 <sup>a</sup>	19.8 ± 1.5 <sup>a</sup>

Any two means in the same column followed by the same letter are not significantly ( $p > 0.05$ ) different from the Duncan's multiple range test.

The neat agar film was very transparent to ultraviolet and visible light. The UV transmittance of the agar film was almost entirely blocked by the addition of resorcinol, which could be attributed to the UV-absorbing ability of the phenolic compound of resorcinol [26]. However, the visible light transmittance (i.e., transparency) of the agar film was not affected by the resorcinol addition. On the other hand, the addition of AgNPs significantly decreased the transmittance at 660 nm (T<sub>660</sub>) depending on the concentration, mainly because the light-impermeable nanoparticles prevent the passage of light. A similar effect of light transmittance by AgNPs was observed in the agar/AgNP nanocomposite film [45].

### 3.2. Morphology and Chemical Structure

The microstructure results are shown in Figure 2. The neat agar and Agar/Res composite films showed a smooth, dense surface without pores and cracks. The Agar/Res/AgNP composite films showed an even distribution of AgNPs in the polymer matrix; however, some aggregation of AgNPs was observed when large amounts of AgNPs (1.5 wt%) were

incorporated. A similar morphology was also observed in carrageen-based films with AgNPs [46].

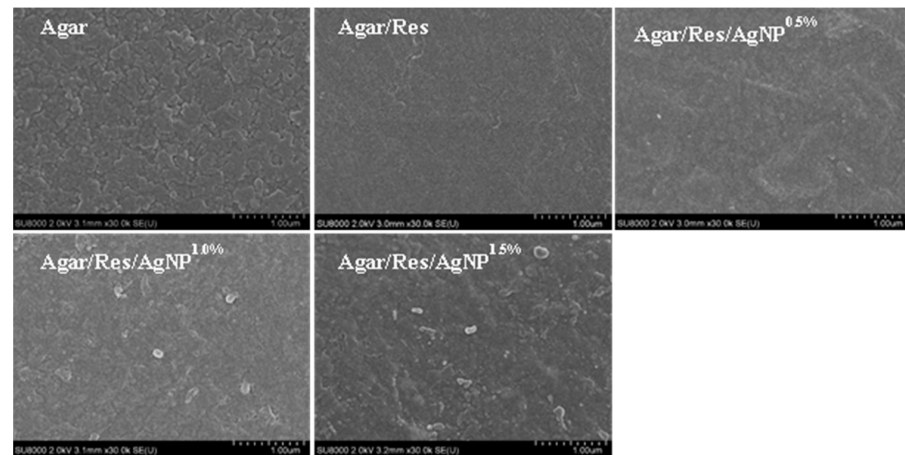


Figure 2. SEM images of the agar-based composite films.

The FTIR spectra of the films are shown in Figure 3. A broad absorption band of  $3276\text{ cm}^{-1}$  was found in all films due to the hydroxyl group's stretching vibration [47]. The peaks at  $2940$  and  $2887\text{ cm}^{-1}$  were due to the C–H stretching [33]. The peak at  $1651\text{ cm}^{-1}$  was ascribed to the stretching vibration of the conjugated peptide bond [48]. The peak at  $1372\text{ cm}^{-1}$  was attributed to an ester sulfate group [49]. The film showed characteristic absorption peaks at  $1035$  and  $932\text{ cm}^{-1}$ , ascribed to the C=O stretching group of 3,6-anhydro-D-galactose [50]. Similar characteristic absorption peaks were observed for the Agar/Res and Agar/Res/AgNP composite films for the neat agar film, suggesting no new chemical bonds were created between the agar, resorcinol, and AgNPs. The main interactions in these composite films are probably physical interactions, such as H bonding and van der Waals forces [51].

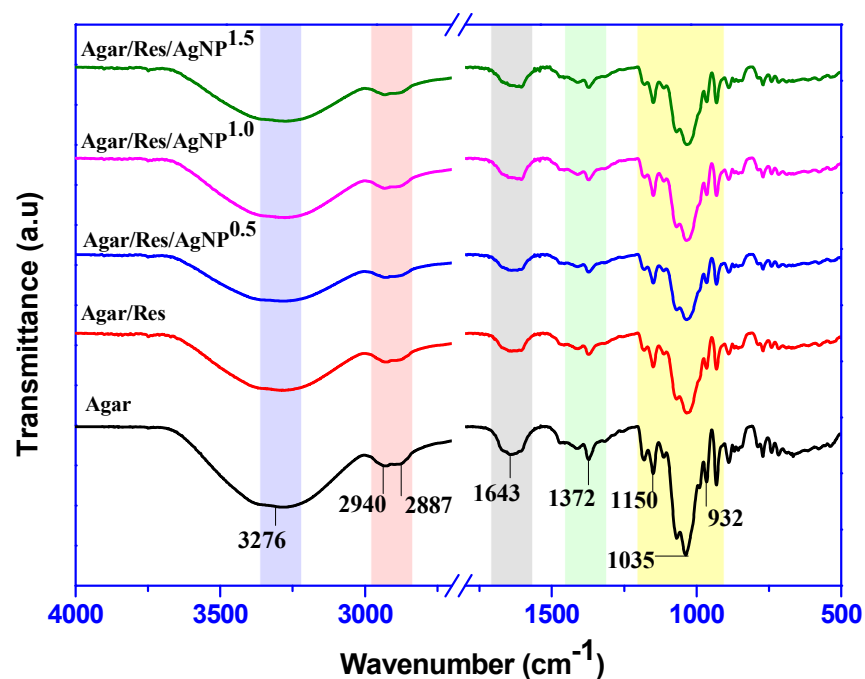


Figure 3. FTIR spectra of the agar-based composite films.

### 3.3. Mechanical Properties

The mechanical properties of the agar-based films are presented in Table 2. The thickness of the agar film was  $48.9 \pm 1.8 \mu\text{m}$  and was not significantly changed by the addition of resorcinol and AgNPs. The TS of the agar film was  $40.6 \pm 4.0 \text{ MPa}$ , and it increased with the addition of resorcinol and AgNPs. In particular, the addition of AgNP enhanced the TS of the film depending on the concentration and reached  $47.4 \pm 2.7 \text{ MPa}$  when 1.5 wt% of AgNPs was added. The increased strength of the composite film was attributed to the interfacial interaction between film matrix and nanoparticles through H-bonding and van der Waals interaction [52,53]. The rigidity (EM) of the agar film also increased by adding resorcinol and AgNP, but the flexibility (EB) of the film decreased gradually as the AgNP concentration increased. In general, as the film becomes more rigid, the mobility of the polymer chains is inhibited, reducing its flexibility. A similar effect of the mechanical properties of agar-based films was observed when AgNPs were incorporated [34].

**Table 2.** Mechanical properties, WVP, and WCA of the agar-based composite films.

Films	Thickness ( $\mu\text{m}$ )	TS (MPa)	EB (%)	EM (GPa)	WVP ( $\times 10^{-9} \text{ g}\cdot\text{m}/\text{m}^2\cdot\text{Pa}\cdot\text{s}$ )	WCA (deg.)
Agar	$48.9 \pm 1.8^a$	$40.6 \pm 4.0^a$	$16.4 \pm 3.5^b$	$1.0 \pm 0.1^a$	$1.0 \pm 0.1^c$	$46.2 \pm 2.2^b$
Agar/Res	$47.8 \pm 2.6^a$	$42.4 \pm 3.6^{ab}$	$16.1 \pm 2.6^b$	$1.2 \pm 0.1^b$	$1.0 \pm 0.1^c$	$33.0 \pm 1.9^a$
Agar/Res/AgNP <sup>0.5%</sup>	$45.9 \pm 1.6^a$	$43.1 \pm 4.5^{ab}$	$13.8 \pm 2.5^a$	$1.3 \pm 0.1^c$	$0.9 \pm 0.1^b$	$54.1 \pm 2.3^c$
Agar/Res/AgNP <sup>1%</sup>	$47.9 \pm 6.7^a$	$44.8 \pm 4.5^{bc}$	$13.2 \pm 2.3^a$	$1.3 \pm 0.1^c$	$0.9 \pm 0.1^b$	$64.4 \pm 1.2^d$
Agar/Res/AgNP <sup>1.5%</sup>	$46.6 \pm 2.0^a$	$47.4 \pm 2.7^c$	$12.2 \pm 1.8^a$	$1.4 \pm 0.1^c$	$0.8 \pm 0.1^a$	$66.7 \pm 1.3^e$

Any two means in the same column followed by the same letter are not significantly ( $p > 0.05$ ) different from the Duncan's multiple range test.

### 3.4. Water Vapor Permeability (WVP) and Water Contact Angle (WCA)

The WVP of the agar-based film is shown in Table 2. The WVP of the neat agar film was  $1.0 \times 10^{-9} \text{ g}\cdot\text{m}/\text{m}^2\cdot\text{Pa}\cdot\text{s}$ , which is consistent with the previously reported values of the agar film [38]. The addition of resorcinol did not affect the WVP of the film, but the addition of AgNPs significantly decreased the WVP. The increased water vapor barrier properties of the Agar/Res/AgNP films (i.e., reduced WVP) were probably due to the tortuous path of water vapor permeation [44]. Moreover, the increased hydrogen bonding is thought to decrease the free volume of the film matrix and prevent the permeation of water vapor [16].

The WCA is usually used to check the surface hydrophilicity or hydrophobicity of the film. The WCA of the agar-based films is also shown in Table 2. The WCA of the neat agar film was  $46.2 \pm 2.2^\circ$ , indicating the agar film is hydrophilic. The addition of resorcinol reduced the WCA of the agar film significantly to  $33.0 \pm 1.9^\circ$  due to the hydrophilic nature of resorcinol [26]. A similar decrease in the WCA of agar film was observed when grapefruit seed extract containing phenolic compounds was incorporated [54]. Conversely, the addition of AgNPs pointedly increased the WCA of the agar film, and the addition of 1.5 wt% AgNPs increased it to  $66.7^\circ$ . The increase in the hydrophobicity of the agar film by the addition of AgNPs was due to the hydrophobicity of the nanoparticles [55]. Generally, a biopolymer film with a WCA higher than  $65^\circ$  is considered a hydrophobic film [48]. The increased hydrophobicity of the agar film is desirable for high moisture food packaging applications.

### 3.5. Thermal Stability

The thermograms of the films are shown in Figure 4. The first weight loss of the films occurred in the range of 60–120 °C with a maximum of around 90 °C due to the evaporation of moisture. The second weight loss was observed in the range of 230–360 °C due to



the thermal decomposition of glycerol and polymer matrix [56]. The DTG thermograms showed two different maximum decomposition temperatures: 233–244 °C for glycerol decomposition and 293–299 °C for polymer decomposition. The glycerol decomposition temperature of the agar film was slightly increased by AgNP addition, and the glycerol decomposition peak almost disappeared when 1.5 wt% of AgNPs was added. On the other hand, the polymer decomposition peak was not clear in the neat agar film. Still, the peak became more distinct when AgNPs were added, and the maximum decomposition temperature increased as the AgNP concentration increased. These results indicate that the addition of AgNPs increased the thermal stability of the agar film. This increase in thermal stability may be related to the crystal structure of AgNPs because more energy is required to break down films with high crystallinity [57,58]. Davidović et al. (2019) also reported an increase in the thermal stability of agar-based films by adding AgNPs and magnesium ions [36]. At 600 °C, the residual char content of the film was ~25–32%.

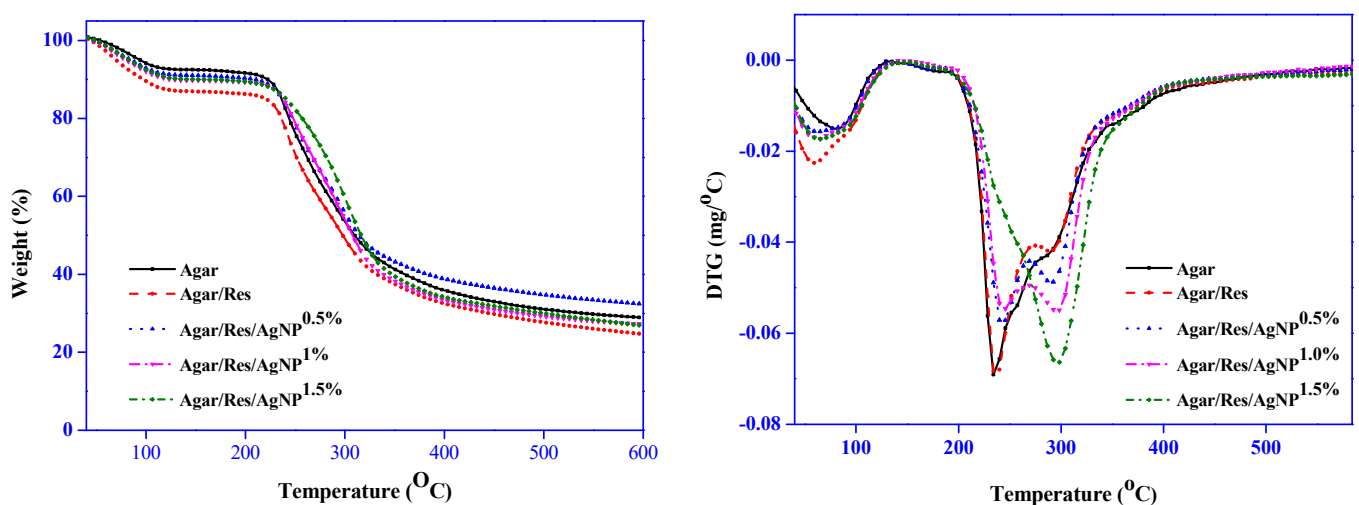


**Figure 4.** TGA and DTG thermograms of the agar-based composite films.

### 3.6. Antioxidant Activity

The antioxidant activity results are shown in Figure 5. The neat agar film showed negligible antioxidant activity in the DPPH assay and some antioxidant activity in the ABTS assay. The antioxidant activity of the neat agar film was due to the sulfate group of the agar [59,60]. Current observations on the antioxidant activity of agar-based films are similar to previously published results [46]. Yet, the antioxidant activity of agar film was pointedly amplified when resorcinol was added. The Agar/Res film exhibited ABTS radical scavenging activity of 99% and DPPH radical scavenging activity of 38%. The higher antioxidant activity in the ABTS method than in the DPPH method was due to the different solvent systems used in the analysis, namely an aqueous solution of the former method and a methanol solution of the latter method [61]. However, AgNP addition did not affect the antioxidant activity of the composite film (Agar/Res/AgNP film), but rather a slight decrease in antioxidant activity was observed compared to the Agar/Res film. These results indicate that the antioxidant activity of the composite film comes mainly from resorcinol. The antioxidant activity of resorcinol-added films is due to the phenolic components existing in resorcinol acting as potent hydrogen donors [62,63]. Since the phenolic compound is water-soluble, the antioxidant activity of the resorcinol-containing film was greater in the ABTS method than in the DPPH method.

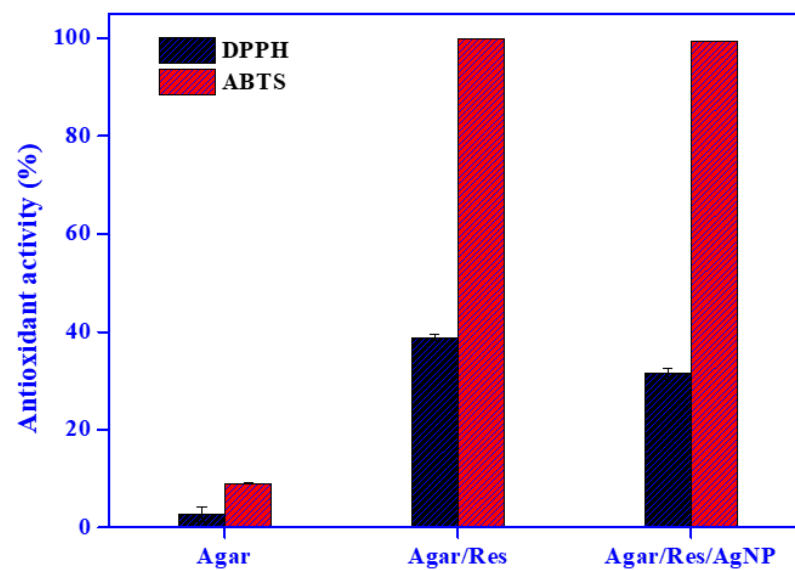


**Figure 5.** Antioxidant activity of the agar-based composite films determined by the DPPH and ABTS methods.

### 3.7. Antimicrobial Activity

The antimicrobial activity results are shown in Figure 6. The neat agar film and Agar/Res film did not show any antimicrobial activity against Gram-positive and Gram-negative bacteria, showing growth similar to that of the control group. However, AgNP-added films showed significant antimicrobial activity against all test bacteria. The antimicrobial activity depended on the concentration of AgNPs present in the agar-based films. These results indicate that the antimicrobial activity of the composite film comes mainly from AgNPs. In addition, the antimicrobial activity of the Agar/Res/AgNP composite film was greater against *E. coli* (Gram-negative) than against *L. monocytogenes* (Gram-positive). Agar/Res/AgNP composite films containing 1.5 wt% AgNPs inhibited *E. coli* completely at 6 h incubation, but stopped the growth of *L. monocytogenes* at 9 h. The difference in antimicrobial activity of AgNPs between the test bacteria is mainly due to the difference in the thickness and structure of the cell wall of Gram-positive and Gram-negative bacteria [64]. The thin peptidoglycan layer of Gram-negative bacteria facilitates the penetration of AgNPs than Gram-positive bacteria with thick cell wall structures, making them more susceptible to AgNPs [65]. Similar antimicrobial activity has been observed in AgNP-incorporated carrageenan films [16].

Although the broad-spectrum antimicrobial activity of AgNPs is well known, its antibacterial mechanism has not been elucidated. However, several possible mechanisms for the antibacterial action of AgNPs have been proposed. One of them is that the antibacterial activity of AgNPs is due to the destruction of the cell membrane of microorganisms by AgNPs [66]. Kanmani and Rhim (2014) reported that AgNPs penetrate bacteria and form free radicals, inhibiting bacterial metabolic processes and killing microorganisms [67]. In addition, it has been suggested that the interaction between positively charged AgNPs and negatively charged bacterial cell walls results in cell death [60]. Further studies are needed to fully understand the antimicrobial activity of AgNPs and the safety of AgNPs for use in active food packaging applications [68].

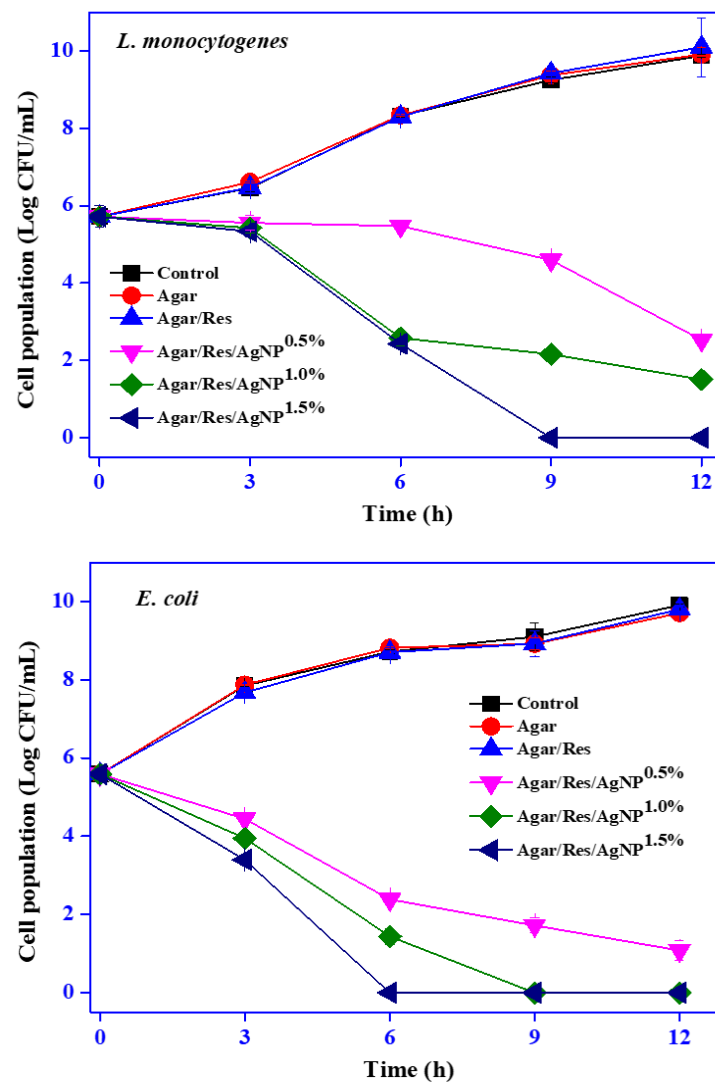


Figure 6. Antimicrobial activity of the agar-based composite films against *E. coli* and *L. monocytogenes*.

#### 4. Conclusions

Agar-based functional films were prepared in situ by using resorcinol for reducing  $\text{AgNO}_3$  and agar to stabilize AgNPs and polymer matrices. The incorporation of resorcinol-mediated AgNPs had a significant impact on the optical, structural, and mechanical properties of the agar-based films. In particular, the addition of AgNPs significantly enhanced the mechanical strength, surface hydrophobicity, and thermal stability of the film and provided strong antibacterial activity. The addition of resorcinol improved the UV-barrier property and antioxidant activity of the film. The Agar/Res/AgNP composite film completely inhibited the growth of foodborne pathogenic bacteria, *E. coli* and *L. monocytogenes*. The Agar/Res/AgNP composite films with enhanced physical and functional properties are likely to be used in active packaging applications to improve the shelflife of foods.

**Supplementary Materials:** The following supporting information can be downloaded at: <https://www.mdpi.com/article/10.3390/jcs6050124/s1>.

**Author Contributions:** Conceptualization, Y.-J.B. and J.-W.R.; methodology, Y.-J.B.; software, Y.-J.B.; validation, Y.-J.B., S.R. and J.-W.R.; formal analysis, Y.-J.B.; investigation, S.R.; resources, J.-W.R.; data curation, Y.-J.B.; writing—original draft preparation, Y.-J.B.; writing—review and editing, S.R. and J.-W.R.; visualization, S.R. and J.-W.R.; supervision, J.-W.R.; project administration, J.-W.R.; funding acquisition, J.-W.R. All authors have read and agreed to the published version of the manuscript.

**Funding:** This work was supported by the National Research Foundation of Korea (NRF) grant funded by the Korean government (MSIT) (No. 2022R1A2B02001422).

**Institutional Review Board Statement:** Not applicable.

**Informed Consent Statement:** Not applicable.

**Data Availability Statement:** Not applicable.

**Conflicts of Interest:** The authors declare that there is no conflict of interest.

## References

1. Geyer, R.; Jambeck, J.R.; Law, K.L. Production, use, and fate of all plastics ever made. *Sci. Adv.* **2017**, *3*, e1700782. [[CrossRef](#)] [[PubMed](#)]
2. Siracusa, V. Microbial degradation of synthetic biopolymers waste. *Polymers* **2019**, *11*, 1066. [[CrossRef](#)]
3. Chausali, N.; Saxena, J.; Prasad, R. Recent trends in nanotechnology applications of bio-based packaging. *J. Agric. Food Res.* **2022**, *7*, 100257. [[CrossRef](#)]
4. Roy, S.; Rhim, J.-W. New insight into melanin for food packaging and biotechnology applications. *Crit. Rev. Food Sci. Nutr.* **2021**. [[CrossRef](#)] [[PubMed](#)]
5. Priyadarshi, R.; Roy, S.; Ghosh, T.; Biswas, D.; Rhim, J.-W. Antimicrobial nanofillers reinforced biopolymer composite films for active food packaging applications—a review. *Sustain. Mater. Technol.* **2021**, e00353, *in press*. [[CrossRef](#)]
6. Ashfaq, A.; Khurshed, N.; Fatima, S.; Anjum, Z.; Younis, K. Application of nanotechnology in food packaging: Pros and Cons. *J. Agric. Food Res.* **2022**, *7*, 100270. [[CrossRef](#)]
7. Roy, S.; Priyadarshi, R.; Ezati, P.; Rhim, J.-W. Curcumin and its uses in active and smart food packaging applications—A comprehensive review. *Food Chem.* **2022**, *375*, 131885. [[CrossRef](#)] [[PubMed](#)]
8. Yan, M.R.; Hsieh, S.; Ricacho, N. Innovative food packaging, food quality and safety, and consumer perspectives. *Processes* **2022**, *10*, 747. [[CrossRef](#)]
9. Siracusa, V.; Blanco, I.; Romani, S.; Tylewicz, U.; Dalla Rosa, M. Gas permeability and thermal behavior of polypropylene films used for packaging minimally processed fresh-cut potatoes: A case study. *J. Food Sci.* **2012**, *77*, E264–E272. [[CrossRef](#)]
10. Han, W.; Yu, Y.; Li, N.; Wang, L. Application and safety assessment for nanocomposite materials in food packaging. *Chin. Sci. Bull.* **2011**, *56*, 1216–1225. [[CrossRef](#)]
11. Kim, H.J.; Roy, S.; Rhim, J.-W. Gelatin/agar-based color-indicator film integrated with *Clitoria ternatea* flower anthocyanin and zinc oxide nanoparticles for monitoring freshness of shrimp. *Food Hydrocoll.* **2022**, *124*, 107294. [[CrossRef](#)]
12. Roy, S.; Rhim, J.-W. Gelatin/cellulose nanofiber-based functional films added with mushroom-mediated sulfur nanoparticles for active packaging applications. *J. Nanostructure Chem.* **2022**, 1–22. [[CrossRef](#)]
13. Alfei, S.; Marengo, B.; Zuccari, G. Nanotechnology application in food packaging: A plethora of opportunities versus pending risks assessment and public concerns. *Food Res. Int.* **2020**, *137*, 109664. [[CrossRef](#)] [[PubMed](#)]
14. Nile, S.H.; Baskar, V.; Selvaraj, D.; Nile, A.; Xiao, J.; Kai, G. Nanotechnologies in food science: Applications, recent trends, and future perspectives. *Nano-Micro Lett.* **2020**, *12*, 45. [[CrossRef](#)]
15. Rao, S.Q.; Zhang, R.Y.; Chen, R.; Gao, Y.J.; Gao, L.; Yang, Z.Q. Nanoarchitectonics for enhanced antibacterial activity with *Lactobacillus buchneri* S-layer proteins-coated silver nanoparticles. *J. Hazard. Mater.* **2022**, *426*, 128029. [[CrossRef](#)]
16. Roy, S.; Shankar, S.; Rhim, J.-W. Melanin-mediated synthesis of silver nanoparticle and its use for the preparation of carrageenan-based antibacterial films. *Food Hydrocoll.* **2019**, *88*, 237–246. [[CrossRef](#)]
17. Rhim, J.-W.; Wang, L.-F.; Lee, Y.; Hong, S.-I. Preparation and characterization of bio-nanocomposite films of agar and silver nanoparticles: Laser ablation method. *Carbohydr. Polym.* **2014**, *103*, 456–465. [[CrossRef](#)]
18. Sau, S.; Kundu, S. Variation in structure and properties of poly (vinyl alcohol) (PVA) film in the presence of silver nanoparticles grown under heat treatment. *J. Mol. Struct.* **2022**, *1250*, 131699. [[CrossRef](#)]
19. Kalishwaralal, K.; Deepak, V.; Pandian, S.R.K.; Kottaisamy, M.; BarathManiKanth, S.; Kartikeyan, B.; Gurunathan, S. Biosynthesis of silver and gold nanoparticles using *Brevibacterium casei*. *Colloids Surf. B Biointerfaces* **2010**, *77*, 257–262. [[CrossRef](#)]
20. Ameen, F. Optimization of the synthesis of fungus-mediated bi-metallic Ag-Cu nanoparticles. *Appl. Sci.* **2022**, *12*, 1384. [[CrossRef](#)]
21. Hashemi, Z.; Shirzadi-Ahodashti, M.; Mortazavi-Derazkola, S.; Ebrahimzadeh, M.A. Sustainable biosynthesis of metallic silver nanoparticles using barberry phenolic extract: Optimization and evaluation of photocatalytic, in vitro cytotoxicity, and antibacterial activities against multidrug-resistant bacteria. *Inorg. Chem. Commun.* **2022**, *139*, 109320. [[CrossRef](#)]
22. Roy, S.; Das, T.K. Effect of biosynthesized silver nanoparticles on the growth and some biochemical parameters of *Aspergillus foetidus*. *J. Environ. Chem. Eng.* **2016**, *4*, 1574–1583. [[CrossRef](#)]
23. Krishnaraj, C.; Jagan, E.; Rajasekar, S.; Selvakumar, P.; Kalaichelvan, P.; Mohan, N. Synthesis of silver nanoparticles using *Acalypha indica* leaf extracts and its antibacterial activity against waterborne pathogens. *Colloids Surf. B Biointerfaces* **2010**, *76*, 50–56. [[CrossRef](#)] [[PubMed](#)]
24. Ghosh, S.; Roy, S.; Naskar, J.; Kole, R.K. Process optimization for biosynthesis of mono and bimetallic alloy nanoparticle catalysts for degradation of dyes in individual and ternary mixture. *Sci. Rep.* **2020**, *10*, 277. [[CrossRef](#)]

25. Ghosh, S.; Rana, D.; Sarkar, P.; Roy, S.; Kumar, A.; Naskar, J.; Kole, R.K. Ecological safety with multifunctional applications of biogenic mono and bimetallic (Au-Ag) alloy nanoparticles. *Chemosphere* **2022**, *288*, 132585. [[CrossRef](#)]
26. Bang, Y.-J.; Shankar, S.; Rhim, J.-W. In situ synthesis of multi-functional gelatin/resorcinol/silver nanoparticles composite films. *Food Packag. Shelf Life* **2019**, *22*, 100399. [[CrossRef](#)]
27. Jeevan Prasad Reddy, D.; Varada Rajulu, A.; Arumugam, V.; Naresh, M.; Muthukrishnan, M. Effects of resorcinol on the mechanical properties of soy protein isolate films. *J. Plast. Film. Sheeting* **2009**, *25*, 221–233. [[CrossRef](#)]
28. Kumar, A.; Aerry, S.; Goia, D.V. Preparation of concentrated stable dispersions of uniform Ag nanoparticles using resorcinol as reductant. *J. Colloid Interface Sci.* **2016**, *470*, 196–203. [[CrossRef](#)]
29. Blanco, I. Lifetime prediction of polymers: To bet, or not to bet—Is this the question? *Materials* **2018**, *11*, 1383. [[CrossRef](#)]
30. Blanco, I. Lifetime prediction of food and beverage packaging wastes. *J. Therm. Anal. Calorim.* **2016**, *125*, 809–816. [[CrossRef](#)]
31. Akhter, R.; Masoodi, F.; Wani, T.A.; Rather, S.A. Functional characterization of biopolymer-based composite film: Incorporation of natural essential oils and antimicrobial agents. *Int. J. Biol. Macromol.* **2019**, *137*, 1245–1255. [[CrossRef](#)]
32. Mostafavi, F.S.; Zaeim, D. Agar-based edible films for food packaging applications—A review. *Int. J. Biol. Macromol.* **2020**, *159*, 1165–1176. [[CrossRef](#)] [[PubMed](#)]
33. Roy, S.; Kim, H.J.; Rhim, J.-W. Synthesis of carboxymethyl cellulose and agar-based multifunctional films reinforced with cellulose nanocrystals and shikonin. *ACS Appl. Polym. Mater.* **2021**, *3*, 1060–1069. [[CrossRef](#)]
34. Wang, L.-F.; Rhim, J.-W. Preparation and application of agar/alginate/collagen ternary blend functional food packaging films. *Int. J. Biol. Macromol.* **2015**, *80*, 460–468. [[CrossRef](#)] [[PubMed](#)]
35. Giménez, B.; De Lacey, A.L.; Pérez-Santín, E.; López-Caballero, M.; Montero, P. Release of active compounds from agar and agar–gelatin films with green tea extract. *Food Hydrocoll.* **2013**, *30*, 264–271. [[CrossRef](#)]
36. Davidović, S.; Lazić, V.; Miljković, M.; Gordić, M.; Sekulić, M.; Marinović-Cincović, M.; Nedeljković, J.M. Antibacterial ability of immobilized silver nanoparticles in agar-agar films co-doped with magnesium ions. *Carbohydr. Polym.* **2019**, *224*, 115187. [[CrossRef](#)]
37. Gudadhe, J.A.; Yadav, A.; Gade, A.; Marcato, P.D.; Durán, N.; Rai, M. Preparation of an agar-silver nanoparticles (A-AgNp) film for increasing the shelf-life of fruits. *IET Nanobiotechnol.* **2014**, *8*, 190–195. [[CrossRef](#)]
38. Rhim, J.-W.; Wang, L.; Hong, S. Preparation and characterization of agar/silver nanoparticles composite films with antimicrobial activity. *Food Hydrocoll.* **2013**, *33*, 327–335. [[CrossRef](#)]
39. Vejdán, A.; Ojagh, S.M.; Adeli, A.; Abdollahi, M. Effect of TiO<sub>2</sub> nanoparticles on the physico-mechanical and ultraviolet light barrier properties of fish gelatin/agar bilayer film. *LWT-Food Sci. Technol.* **2016**, *71*, 88–95. [[CrossRef](#)]
40. Suresh, S.; Srivastava, V.C.; Mishra, I.M. Adsorption of catechol, resorcinol, hydroquinone, and their derivatives: A review. *Int. J. Energy Environ. Eng.* **2012**, *3*, 32. [[CrossRef](#)]
41. Ponsanti, K.; Tangnorawich, B.; Ngernyuang, N.; Pechyen, C. A flower shape-green synthesis and characterization of silver nanoparticles (AgNPs) with different starch as a reducing agent. *J. Mater. Res. Technol.* **2020**, *9*, 11003–11012. [[CrossRef](#)]
42. Bousalem, N.; Benmansour, K.; Ziani Cherif, H. Synthesis and characterization of antibacterial silver-alginate-chitosan bio-nanocomposite films using UV irradiation method. *Mater. Technol.* **2017**, *32*, 367–377. [[CrossRef](#)]
43. Ahmed, S.; Saifullah Ahmad, M.; Swami, B.L.; Ikram, S. Green synthesis of silver nanoparticles using *Azadirachta indica* aqueous leaf extract. *J. Radiat. Res. Appl. Sci.* **2016**, *9*, 1–7. [[CrossRef](#)]
44. Roy, S.; Das, T.K. Biosynthesis of silver nanoparticles by *Aspergillus foetidus*: Optimization of physicochemical parameters. *Nanosci. Nanotechnol. Lett.* **2014**, *6*, 181–189. [[CrossRef](#)]
45. Bahrami, A.; Mokarram, R.R.; Khiabani, M.S.; Ghanbarzadeh, B.; Salehi, R. Physico-mechanical and antimicrobial properties of tragacanth/hydroxypropyl methylcellulose/beeswax edible films reinforced with silver nanoparticles. *Int. J. Biol. Macromol.* **2019**, *129*, 1103–1112. [[CrossRef](#)]
46. Roy, S.; Rhim, J.-W. Agar-based antioxidant composite films incorporated with melanin nanoparticles. *Food Hydrocoll.* **2019**, *94*, 391–398. [[CrossRef](#)]
47. Wu, Y.; Geng, F.; Chang, P.R.; Yu, J.; Ma, X. Effect of agar on the microstructure and performance of potato starch film. *Carbohydr. Polym.* **2009**, *76*, 299–304. [[CrossRef](#)]
48. Roy, S.; Rhim, J.-W.; Jaiswal, L. Bioactive agar-based functional composite film incorporated with copper sulfide nanoparticles. *Food Hydrocoll.* **2019**, *93*, 156–166. [[CrossRef](#)]
49. Volery, P.; Besson, R.; Schaffer-Lequart, C. Characterization of commercial carrageenans by Fourier transform infrared spectroscopy using single-reflection attenuated total reflection. *J. Agric. Food Chem.* **2004**, *52*, 7457–7463. [[CrossRef](#)]
50. Gómez-Ordóñez, E.; Rupérez, P. FTIR-ATR spectroscopy as a tool for polysaccharide identification in edible brown and red seaweeds. *Food Hydrocoll.* **2011**, *25*, 1514–1520. [[CrossRef](#)]
51. Li, X.; Li, H.; Wang, X.; Xu, D.; You, T.; Wu, Y.; Xu, F. Facile in situ fabrication of ZnO-embedded cellulose nanocomposite films with antibacterial properties and enhanced mechanical strength via hydrogen bonding interactions. *Int. J. Biol. Macromol.* **2021**, *183*, 760–771. [[CrossRef](#)] [[PubMed](#)]
52. Ezati, P.; Roy, S.; Rhim, J.-W. Pectin/gelatin-based bioactive composite films reinforced with sulfur functionalized carbon dots. *Colloids Surf. A Physicochem. Eng. Asp.* **2022**, *636*, 128123. [[CrossRef](#)]
53. Hou, X.; Xue, Z.; Liu, J.; Yan, M.; Xia, Y.; Ma, Z. Characterization and property investigation of novel eco-friendly agar/carrageenan/TiO<sub>2</sub> nanocomposite films. *J. Appl. Polym. Sci.* **2019**, *136*, 47113. [[CrossRef](#)]

54. Kanmani, P.; Rhim, J.-W. Antimicrobial and physical-mechanical properties of agar-based films incorporated with grapefruit seed extract. *Carbohydr. Polym.* **2014**, *102*, 708–716. [[CrossRef](#)] [[PubMed](#)]
55. Kraśniewska, K.; Galus, S.; Gniewosz, M. Biopolymers-based materials containing silver nanoparticles as active packaging for food applications—A review. *Int. J. Mol. Sci.* **2020**, *21*, 698. [[CrossRef](#)]
56. Mallakpour, S.; Rashidimoghadam, S. Application of ultrasonic irradiation as a benign method for production of glycerol plasticized-starch/ascorbic acid functionalized MWCNTs nanocomposites: Investigation of methylene blue adsorption and electrical properties. *Ultrason. Sonochem.* **2018**, *40*, 419–432. [[CrossRef](#)]
57. Kadam, D.; Momin, B.; Palamthodi, S.; Lele, S. Physicochemical and functional properties of chitosan-based nanocomposite films incorporated with biogenic silver nanoparticles. *Carbohydr. Polym.* **2019**, *211*, 124–132. [[CrossRef](#)]
58. Roy, S.; Rhim, J.-W. Preparation of antimicrobial and antioxidant gelatin/curcumin composite films for active food packaging application. *Colloids Surf. B Biointerfaces* **2020**, *188*, 110761. [[CrossRef](#)]
59. Chen, H.; Yan, X.; Zhu, P.; Lin, J. Antioxidant activity and hepatoprotective potential of agaro-oligosaccharides in vitro and in vivo. *Nutr. J.* **2006**, *5*, 31. [[CrossRef](#)]
60. Wang, J.; Jiang, X.; Mou, H.; Guan, H. Anti-oxidation of agar oligosaccharides produced by agarase from a marine bacterium. *J. Appl. Phycol.* **2004**, *16*, 333–340. [[CrossRef](#)]
61. Łopusiewicz, Ł.; Macieja, S.; Śliwiński, M.; Bartkowiak, A.; Roy, S.; Sobolewski, P. Alginate biofunctional films modified with melanin from watermelon seeds and zinc oxide/silver nanoparticles. *Materials* **2022**, *15*, 2381. [[CrossRef](#)] [[PubMed](#)]
62. Kharat, S.N.; Mendhulkar, V.D. Synthesis, characterization and studies on antioxidant activity of silver nanoparticles using *Elephantopus scaber* leaf extract. *Mater. Sci. Eng. C* **2016**, *62*, 719–724. [[CrossRef](#)] [[PubMed](#)]
63. Subramanian, R.; Subbramaniyan, P.; Raj, V. Antioxidant activity of the stem bark of *Shorea roxburghii* and its silver reducing power. *SpringerPlus* **2013**, *2*, 28. [[CrossRef](#)] [[PubMed](#)]
64. Lee, J.H.; Jeong, D.; Kanmani, P. Study on physical and mechanical properties of the biopolymer/silver based active nanocomposite films with antimicrobial activity. *Carbohydr. Polym.* **2019**, *224*, 115159. [[CrossRef](#)] [[PubMed](#)]
65. Anitha, S.; Brabu, B.; Thiruvadigal, D.J.; Gopalakrishnan, C.; Natarajan, T. Optical, bactericidal, and water repellent properties of electrospun nanocomposite membranes of cellulose acetate and ZnO. *Carbohydr. Polym.* **2012**, *87*, 1065–1072. [[CrossRef](#)]
66. Dai, X.; Li, S.; Li, S.; Ke, K.; Pang, J.; Wu, C.; Yan, Z. High antibacterial activity of chitosan films with covalent organic frameworks immobilized silver nanoparticles. *Int. J. Biol. Macromol.* **2022**, *202*, 407–417. [[CrossRef](#)]
67. Ghetas, H.A.; Abdel-Razek, N.; Shakweer, M.S.; Abotaleb, M.M.; Paray, B.A.; Ali, S.; Khalil, R.H. Antimicrobial activity of chemically and biologically synthesized silver nanoparticles against some fish pathogens. *Saudi J. Biol. Sci.* **2022**, *29*, 1298–1305. [[CrossRef](#)]
68. Zhai, X.; Zhou, S.; Zhang, R.; Wang, W.; Hou, H. Antimicrobial starch/poly(butylene adipate-co-terephthalate) nanocomposite films loaded with a combination of silver and zinc oxide nanoparticles for food packaging. *Int. J. Biol. Macromol.* **2022**, *206*, 298–305. [[CrossRef](#)]